Wideband Rectangular Planar Monopole Antenna for OAM Wave Generation

Nidal Qasem[1†] and Ahmad Alamayreh[2†]
Ne.qasem@ammanu.edu.jo A.amayreh@ammanu.edu.jo
[†] Department of Electronics and Communications Engineering
Al-Ahliyya Amman University, Amman, Jordan

Summary
Generating electromagnetic waves with Orbital Angular Momentum (OAM) properties is a fast-growing research subject in both radio and optics. This paper describes the generation of OAM carrying waves using a circular array of rectangular planar monopole antennas. The proposed design combines simplicity, compactness, and most importantly very wideband of operating frequencies (about 20–160 GHz, bandwidth ratio about 1:8) which makes it suitable for future applications.

Key words:
Antennas, orbital angular momentum, planar metal-plate monopole antenna.

1. Introduction

Wireless communication technology has developed rapidly to meet the demand for high traffic capacities in electronic devices. Fifth Generation (5G) technology utilizes higher-frequency bands in order to provide the large information capacities needed to support multi-Gbps information rates and collect infinite information broadcasts using the latest mobile technology [1, 2]. Prominent technologies include: massive multiple-input multiple-output, co-frequency, co-time, full-duplex, and millimeter-wave (mm-wave) [3-5]. In addition, a new and promising means for enhancing the communications spectrum efficiency appeared after the discovery in the early '90s [6] which showed that electromagnetic waves can possess orthogonal Orbital Angular Momentum (OAM) orders. Since then, there has been significant interest in this OAM property in optics and lately in radio communications [7-10].
The conventional way to generate OAM waves over radio and microwave bands is by Uniform Circular Array (UCA) [11]. The radiating elements of the UCA are usually omnidirectional dipoles. Dipole elements are small in size; therefore, many elements can be installed in the array to produce the desired OAM wave order. This is handy especially for generating large OAM orders where the number of needed dipoles becomes large. However, one typical problem pursuit conventional radio vortex generation using UCA is the limited bandwidth of the diploe elements. The main challenge in new radio communication systems is to design a small-sized antenna with a wideband feature that includes the entire accessible band [12]. Applying OAM-based solutions in the radio band is a challenge by its own as OAM radio waves diverge fast when compared to their counterparts in optics. Thus, having an antenna able to operate at a wide band including high frequencies helps confining the radiation.
In this paper we present an array for OAM generation; the basic elements of the array are rectangular Planar Monopole Antennas (PMAs) that are designed to meet the needs of wireless communication applications: small size, easiness of fabrication, and the wide frequency bandwidth. Among PMAs of various shapes, square/rectangular PMAs are the simplest in geometry and, in addition, their radiation patterns are usually less degraded within the impedance bandwidth [13-15].
The remainder of this paper is organized into the following sections: Section 2 reviews antenna configuration and mechanism. Simulation results are presented in Section 3, and finally, conclusions are drawn in Section 4.

2. Antenna Design

2.1 Rectangular Planar Monopole Antenna (PMA)

Fig. 1 shows the geometry of the proposed rectangular Planar Monopole Antenna (PMA) with a trident-shaped feeding strip mounted above a 10×10 mm^2 ground plane. In this design, the rectangular PMA and the trident-shaped feeding strip are integrated and constructed from a single metal plate (a 0.02 mm thick brass sheet). The rectangular PMA is excited at three feeding points A, B, and C at which the PMA is connected to the trident-shaped (or three-branched) feeding strip. Note also that point B corresponds to the central line of the PMA, while points A and C are symmetrically located at either side of point B.
In this study, all points of the trident-shaped feeding strips are 0.1 mm wide. The trident-shaped feeding strip comprises a central branch (length $h + d$) connected to point B and two side branches of an inverted- L shape connected to points A and C, which are spaced at distance t. Through a via-hole in the ground plane, the central branch is connected to a 50 SMA connector behind the ground plane for signal transmission.

Manuscript received March 5, 2021
Manuscript revised March 20, 2021
https://doi.org/10.22937/IJCSNS.2021.21.3.8

The two side branches are identical in shape (a horizontal length $t/2$ and a vertical length h) and have a height of d above the ground plane. By adjusting the three parameters d, t, and h, a greatly enhanced impedance bandwidth can be achieved for the proposed PMA. For the study with a 2.8×2.4 mm rectangular PMA, the optimal values of d and h are 0.1 and 0.28 mm, respectively, while that of t is 0.9 mm, suggesting that points A and C should be roughly located at positions at a distance of about one-third of the side length L to the left- or right-side edge of the rectangular PMA.

To estimate the lower band-edge frequency of printed PMAs, the standard formulation given for cylindrical PMA can be used with suitable modifications [15]. Equation (1) is calculated for the rectangular PMA [16], for which all dimensions are in millimeters.

$$f_L(GHz) = \frac{72}{L+h+\frac{W}{2\pi}} \quad (1)$$

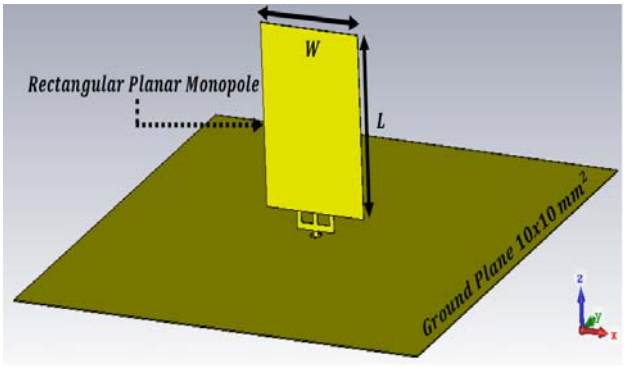

(a) Rectangular PMA.

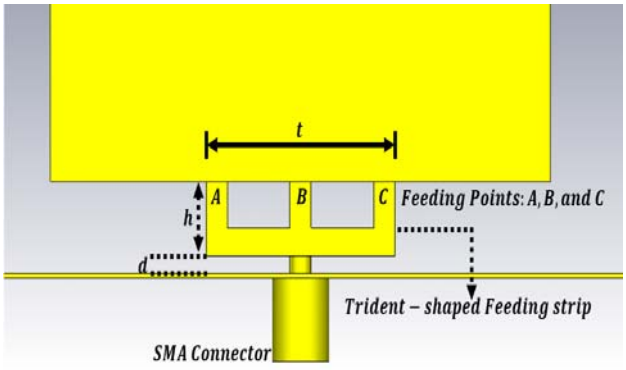

(b) Trident-shaped feeding strip.

Fig. 1 Geometry of the proposed rectangular PMA with a trident-shaped (three-branched) feeding strip.

2.2 Antenna Array for OAM Generation

Electromagnetic waves carrying OAM exhibit helical phase-fronts at propagation. This owes to the azimuthal dependence of the spatial phase distribution $(e^{jl\emptyset})$ of these waves, where l is the OAM order ($l = 0, \pm1, \pm2, \ldots$), and $\emptyset$ is the azimuthal angle. A singularity exists at the wave center along the axis of propagation where the field vanishes due to destructive interference [17].

To generate the phase profile of the OAM wave we arrange an array of the rectangular PMA elements described in the previous section. A sufficient number of elements (N) should be used in the array such that $|l_{max}| \leq {}^{N}/_{2}$ where l_{max} is the maximum OAM order provided by the array. To enforce the phase profile of the OAM wave, the elements are distributed over a circular circumference and each element should be excited by a constant phase offset from its neighbors. The needed phase offset to generate a wave at an order l is $\frac{2\pi}{N}l$.

The complete design is shown in Fig. 2 for an array including 9-radiation elements. This design is theoretically able to produce OAM orders: $\{0, \pm1, \pm2, \pm3, \pm4\}$.

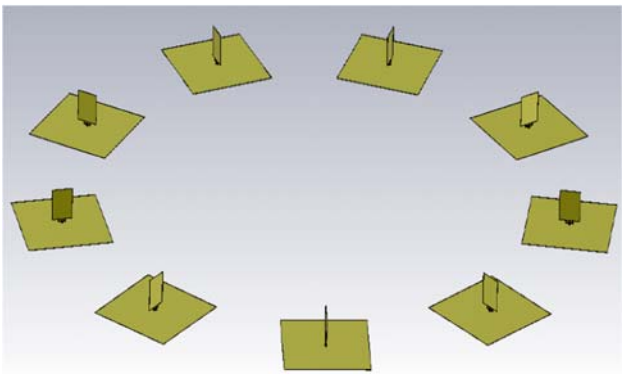

Fig. 2 Circular array configuration including 9-radiation elements.

3. Results and Analysis

Numerical simulation results are presented to demonstrate the design capabilities of the antenna. The first part of the results shows the radiation characteristics of one antenna element. In the second part, multiple elements are arranged to produce an OAM wave. The simulated results are obtained using Computer Simulation Technology (CST) Microwave Studio.

3.1 Rectangular PMA

Prototype of the proposed rectangular PMA with a trident-shaped feeding strip was designed and simulated. The simulated results of the return loss for the case with the proposed trident-shaped feeding strip is shown in Fig. 3. The size of the rectangular PMA was chosen to be 28×24 mm^2, resulting in an impedance bandwidth (10 dB return loss) with a lower edge frequency of approximately 20 GHz. In addition, by selecting the parameters t, h, and d of the feeding strip to be 0.9, 0.28, and 0.1 mm, respectively, the upper edge frequency of the impedance

bandwidth obtained was found to be greater than 160 GHz. This wide impedance bandwidth of 140 GHz makes the proposed antenna very promising for application in the new standard of broadband wireless 5G frequency bands (mm-wave) [18, 19].

The proposed trident-shaped feeding strip was found to have a frequency ratio of 1:8 for the impedance bandwidth obtained. This behavior can be largely attributed to the achievement of a more uniform current distribution in the rectangular PMA [see Fig. 4], like in the three-branch feeding design studied in [14].

The radiation characteristics of the proposed PMA were also analyzed. Fig. 5 plots the simulated radiation pattern at 20 GHz. The gain variations in the azimuthal plane ($x-y$ plane) is greatly dependent on the operating frequency, mainly due to the wide bandwidth of the rectangular PMA. Fig. 6 shows the simulated antenna gain for frequencies across the impedance bandwidth obtained. For frequencies up to approximately 40 GHz, the antenna gain monotonically increases from about 1.5 to 7.0 dBi. For the higher frequency portion of the impedance bandwidth, however, the antenna gain varies over a relatively smaller range of 6.9–7.1 dBi.

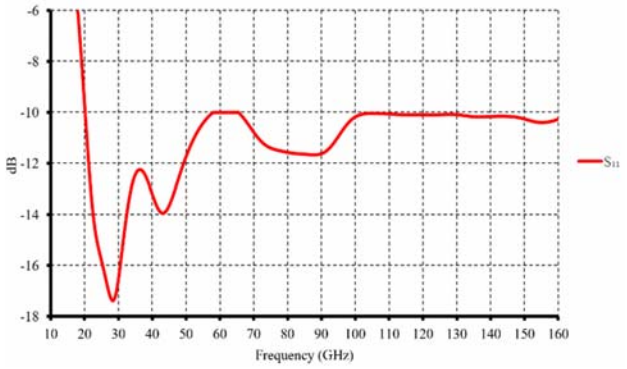

Fig. 3 Simulated return loss for the proposed antenna shown in Fig. 1 with L=28 mm, W=24 mm, t=0.9 mm, h=0.28 mm, and d=0.1 mm.

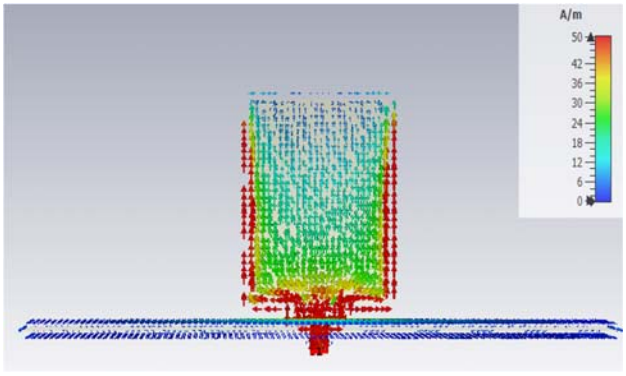

Fig. 4 Simulated surface current distributions for the proposed antenna studied in Fig. 1; f = 20 GHz.

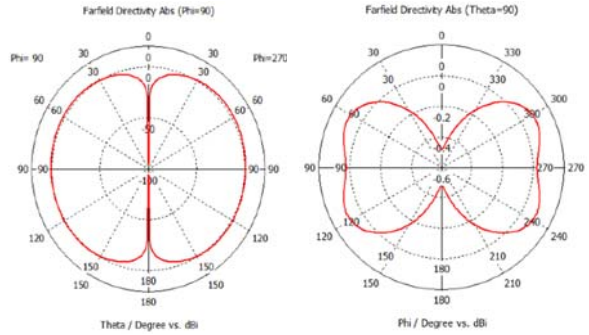

(a) Vertical pattern. (b) Horizontal pattern.

Fig. 5 Simulated far-field directivity radiation patterns at 20 GHz for the proposed antenna studied in Fig. 1.

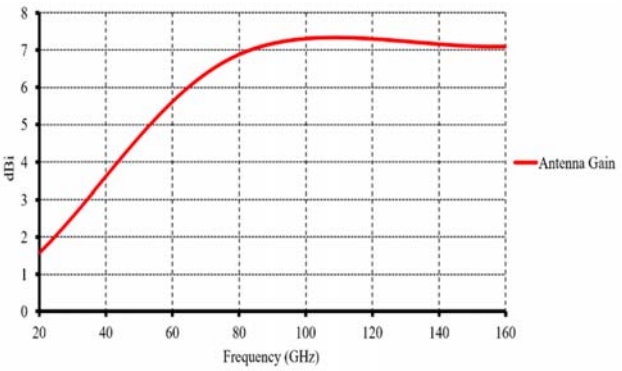

Fig. 6 Simulated antenna gain for the proposed antenna studied in Fig 1.

3.2 OAM

Following the configuration in Fig. 1, 9-radiation elements are placed to form a circular array of radius 25 mm. By appropriate feeding of the elements an OAM wave of certain (up to fourth) order can be generated. The amplitudes of the feeding signals are the same for all elements. The phases of the feeding signals are different and are related to the OAM order as mentioned before.

The OAM properties of the generated wave are demonstrated for the third order (l=3) through phase and amplitude distributions in Fig. 7(a) and Fig. 7(b), respectively. In Fig. 7(b), the change in the amplitude color from blue to red indicates an increase in the field value. The deep blue at the center indicates a null. The phase distribution in Fig. 7 (a) shows three full 2π cycles which agrees with theoretical predictions of OAM waves.

For further comparisons, in Fig. 8 three field plots are obtained in the direction of propagation for the circular array at different frequencies. All cases are for the same OAM order of three and have the same array radius. The beam produced by the low frequency diverges faster. The reduction in the size of the hollow, or null, region in the center of the beam produced by the high frequency is clear evidence of the focusing of the beam attained by increasing the frequency.

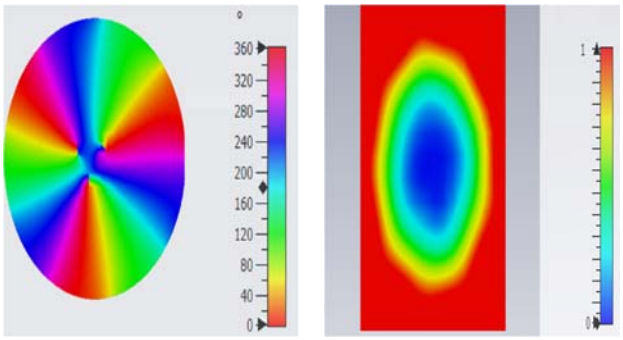

(a) Phase distribution. (b) Normalized amplitude distribution.

Fig. 7 Phase and amplitude distributions of OAM wave of third order (l=3).

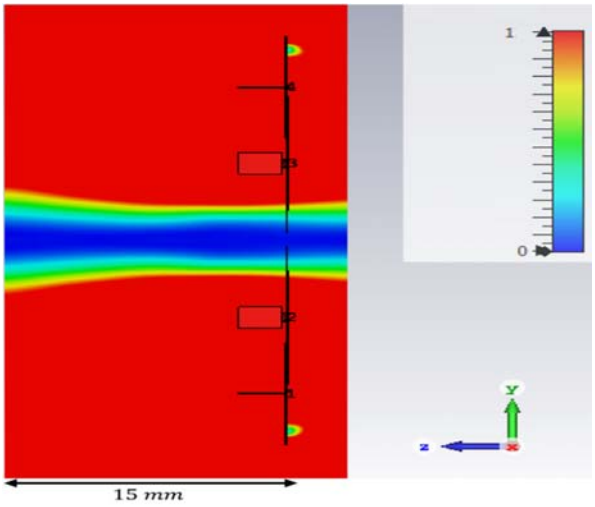

(a) 20 GHz.

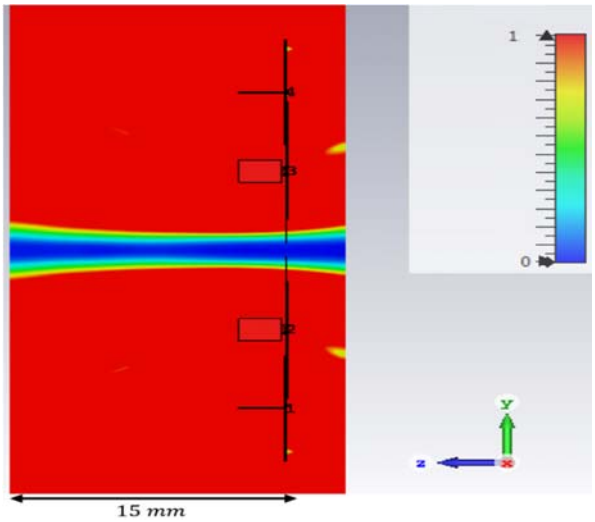

(b) 40 GHz.

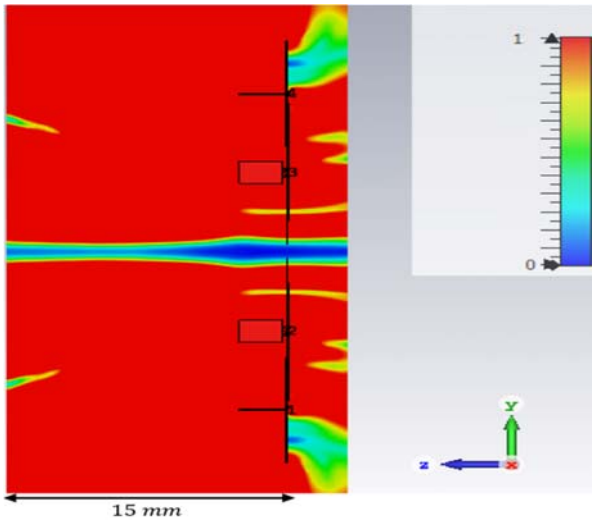

(c) 80 GHz.

Fig. 8 Normalize values for beams in the direction of propagation at three different frequencies for OAM wave of third order (l=3).

4. Conclusion

A rectangular PMA using a trident-shaped feeding strip for achieving a very wide impedance bandwidth has been proposed. The proposed antenna can be easily used for providing OAM-carrying waves in a certain region in space. A very wide impedance bandwidth of about 120 GHz (about 20–160 GHz) has been achieved for the proposed antenna, which makes it very promising for application using OAM techniques.

A transmitting array in the form of the conventional circular array was used. The simulations verified the conclusion drawn in the theoretical derivation: an OAM-carrying wave was generated at the far field; the field phase and amplitude distributions were in agreement with those predicted theoretically for an OAM-carrying wave. Focusing the radiation could be beneficial to limit the interference by operating at a higher frequency within the wide bandwidth supported by the antenna.

References

[1] H. M. Marhoon and N. Qasem, "Simulation and optimization of tuneable microstrip patch antenna for fifth-generation applications based on graphene," International Journal of Electrical and Computer Engineering, vol. 10, no. 5, pp. 5546–5558, 2020, doi: 10.11591/IJECE.V10I5.PP5546-5558.

[2] N. Qasem and H. M. Marhoon, "Simulation and optimization of a tuneable rectangular microstrip patch antenna based on hybrid metal-graphene and FSS superstrate for fifth-generation applications," Telkomnika (Telecommunication Computing Electronics and Control), vol. 18, no. 4, pp. 1719–1730, 2020, doi: 10.12928/telkomnika.v18i4.14988.

[3] W. Cheng, H. Zhang, L. Liang, H. Jing, and Z. Li, "Orbital-Angular-Momentum Embedded Massive MIMO: Achieving Multiplicative Spectrum-Efficiency for mmWave Communications," IEEE Access, vol. 6, pp. 2732–2745, Dec. 2017, doi: 10.1109/ACCESS.2017.2785125.

[4] Nidal Qasem, Emran Ali Aldorgam, and Hadeel Yaseen Alzou'bi, "Overcoming the Influence of Human Shadowing and Obstacles via Modified Building Using Frequency Selective Wallpapers for 60 GHz," Journal of Communication and Computer, vol. 13, no. 2, pp. 90–101, 2016, doi: 10.17265/1548-7709/2016.02.004.

[5] M. Alkhawatra and N. Qasem, "Improving and Extending Indoor Connectivity Using Relay Nodes for 60 GHz Applications," International Journal of Advanced Computer Science and Applications, vol. 7, no. 4, pp. 427–434, 2016, doi: 10.14569/ijacsa.2016.070456.

[6] L. , Allen, M. W. , Beijersbergen, R. J. C. , Spreeuw, and J. P. Woerdman, "Orbital angular momentum of light and the transformation of Laguerre-Gaussian laser modes," Physical review A, vol. 45, no. 11, pp. 8185–8189, 1992.

[7] B. Thidé et al., "Utilization of photon orbital angular momentum in the low-frequency radio domain," Physical Review Letters, vol. 99, no. 8, Aug. 2007, doi: 10.1103/PhysRevLett.99.087701.

[8] K. Liu, Y. Cheng, X. Li, Y. Qin, H. Wang, and Y. Jiang, "Generation of Orbital Angular Momentum Beams for Electromagnetic Vortex Imaging," IEEE Antennas and Wireless Propagation Letters, vol. 15, pp. 1873–1876, 2016, doi: 10.1109/LAWP.2016.2542187.

[9] A. Alamayreh and N. Qasem, "Vortex beam generation in microwave band," Progress In Electromagnetics Research C, vol. 107, no. August 2020, pp. 49–63, 2021, doi: 10.2528/PIERC20082006.

[10] A. Alamayreh, N. Qasem, and J. S. Rahhal, "General configuration MIMO system with arbitrary OAM," Electromagnetics, vol. 40, no. 5, pp. 343–353, 2020, doi: 10.1080/02726343.2020.1780378.

[11] M. Lin, Y. Gao, P. Liu, and J. Liu, "Theoretical Analyses and Design of Circular Array to Generate Orbital Angular Momentum," IEEE Transactions on Antennas and Propagation, vol. 65, no. 7, pp. 3510–3519, 2017, doi: 10.1109/TAP.2017.2700160.

[12] N. Raheem and N. Qasem, "A compact multi-band notched characteristics UWB microstrip patch antenna with a single sheet of graphene," Telkomnika (Telecommunication Computing Electronics and Control), vol. 18, no. 4, pp. 1708–1718, 2020, doi: 10.12928/TELKOMNIKA.V18I4.14942.

[13] E. G. Turitsyna and S. Webb, "Simple design of FBG-based VSB filters for ultra-dense WDM transmission ELECTRONICS LETTERS 20th January 2005," Electronics letters, vol. 41, no. 2, pp. 40–41, 2005, doi: 10.1049/el.

[14] K. L. Wong, C. H. Wu, and S. W. Su, "Ultrawide-band square planar metal-plate monopole antenna with a trident-shaped feeding strip," IEEE Transactions on Antennas and Propagation, vol. 53, no. 4, pp. 1262–1269, 2005, doi: 10.1109/TAP.2005.844430.

[15] N. P. Agrawall, G. Kumar, and K. P. Ray, "Wide-band planar monopole antennas," IEEE Transactions on Antennas and Propagation, vol. 46, no. 2, pp. 294–295, 1998, doi: 10.1109/8.660976.

[16] K. P. Ray, "Design Aspects of Printed Monopole Antennas for Ultra-Wide Band Applications," International Journal of Antennas and Propagation, vol. 2008, pp. 1–8, 2008, doi: 10.1155/2008/713858.

[17] W. Y. Huang, J. L. Li, H. Z. Wang, J. P. Wang, and S. S. Gao, "Vortex Electromagnetic Waves Generated by Using a Laddered Spiral Phase Plate and a Microstrip Antenna," Electromagnetics, vol. 36, no. 2, pp. 102–110, 2016, doi: 10.1080/02726343.2016.1136031.

[18] E. Dahlman, G. Mildh, S. Parkvall, J. Peisa, J. Sachs, and Y. Selén, "5G radio access," Ericsson Review (English Edition), vol. 91, no. 1, pp. 42–47, 2014.

[19] M. Marcus and and B. Pattan, "Millimeter wave propagation: spectrum management implications," Engineering and Technology, vol. 6, no. 2, pp. 54–62, 2005.

Nidal Qasem received his B.Sc. degree in Electronics and Communications Engineering (Honours) from Al-Ahliyya Amman University, Amman, Jordan, in 2004. He obtained his M.Sc. degree in Digital Communication Systems for Networks & Mobile Applications (DSC) in 2006, followed by a Ph.D. in Wireless and Digital Communication Systems, both from Loughborough University, Loughborough, United Kingdom. He currently holds the position of associate professor in the department of Electronics and Communications Engineering at Al-Ahliyya Amman University. His research interests include propagation control in buildings, specifically improving the received power, FSS measurements and designs, antennas, ultra-wide band, orbital angular momentum, and wireless system performance analyses. He is a senior member of the IEEE.

Ahmad Alamayreh received his B.Sc. degree and M.Sc. in Communications Engineering from the University of Jordan, Amman, Jordan, in 2000 and 2002, respectively. He obtained his PhD from the Institut National des Science Appliques de Rennes, Rennes, France, in 2009. He was with France Telecom R&D for three years in Lannion, France. He is currently an assistant professor in the department of Electronics and Communications Engineering at Al-Ahliyya Amman University. His research interests include channel modeling for multiuser MIMO systems.